Journal of The Electrochemical
Society

The Electrochemical Society
Advancing solid state & electrochemical science & technology

Mechanisms of Exclusive Scale Formation in the High Temperature Oxidation of Alloys

To cite this article: William H. Blades *et al* 2022 *J. Electrochem. Soc.* **169** 061501

Journal of The Electrochemical Society, 2022 **169** 061501

Mechanisms of Exclusive Scale Formation in the High Temperature Oxidation of Alloys

William H. Blades,[1] **Elizabeth J. Opila,**[2] **and Karl Sieradzki**[1,z]

[1]Ira A. Fulton School of Engineering, Arizona State University, Tempe, AZ, 85287, United States of America
[2]Department of Materials Science and Engineering, University of Virginia, Charlottesville VA, 22904, United States of America

The high temperature oxidation of alloys is most often considered within the continuum framework developed by C. Wagner. We argue that in order to make progress in understanding exclusive scale formation, one needs to examine the atomic-scale kinetic processes that today are amenable to a variety of experimental, computational and theoretical approaches. In our discussion, we suggest that there is an analogy between the kinetic processes required for exclusive scale formation and thin film layer-by-layer growth. In both cases, the magnitude of the Ehrlich-Schwoebel barrier sets an effective length scale for growth, that if too large, results in three-dimensional rather than lateral island or oxide growth. In this event, exclusive scale formation can only occur if there is a sufficiently large density of oxide nucleation events at the surface of the alloy. We suggest that a suitably identified, dilute alloy component, could serve as a "surfactant" that segregates to the surface and is capable of enhancing the nucleation density.
[DOI: 10.1149/1945-7111/ac751f]

Manuscript submitted March 28, 2022; revised manuscript received May 25, 2022. Published June 10, 2022.

Supplementary material for this article is available online

It has been understood since at least 1965 that lateral growth of oxide precipitates is necessary for the exclusive growth of a protective scale.[1] In this context, exclusive growth refers to the lack of any significant internal oxidation. This means that a large fraction of the protective scale must form during the so-called "transient oxidation" period.[2] In order for lateral growth of oxide precipitates to occur, interfacial diffusion, perpendicular to the oxide/air or metal/oxide interface normal, must be important. It seems straightforward to think of a mechanism for scale formation in terms of a thin film layer-by-layer, island coalescence or step-flow growth analogy [Supplementary material Fig. S1 (available online at stacks.iop.org/JES/169/061501/mmedia)] with two important differences. One is that in a typical thin film growth process the deposition flux is constant, while during scale formation in high temperature (HT) oxidation the flux of the protective scale forming component (B) is a function of the oxidation time. The second is related to the identity of the interfacial diffuser which could correspond to either B and/or oxygen (O) and the subsequent chemical reaction forming nuclei of the protective oxide. Several authors have already qualitatively considered the importance of interfacial diffusion and various aspects of thin film growth processes in the high temperature HT oxidation of both elemental metals and alloys.[3–6]

Almost independent of the alloy composition, it seems that there is always enough of the passivating component available to "quickly" diffuse to the relevant interface for scale formation. Consider an alloy at a composition of A_pB_{1-p} for which, as an illustrative example, a mole fraction of $B \approx 0.5$ is required for scale formation. Diffusion of B from from a depth h (measured as the number of monolayers) will bring the surface composition of B to $1 - p^h$.[7] For $p = 0.95$, diffusion of B from the first 14 atomic layers will bring the surface composition of the B-component to 0.51. Assuming that the relevant interface acts as an instantaneous sink for the B-component, this occurs over time scales of seconds. In the case of Ag-In alloys for which $D_{In} \approx 2.5 \times 10^{-11}$ cm^{2}s^{-1} at 550 °C,[8] it takes less than one second for this to occur. We conclude that bulk diffusion of B is not rate-limiting, if an exclusive scale forms during transient oxidation. Rather, the process determining the rate of scale formation is most likely related to mixed kinetics involving nucleation and the lateral growth of oxide precipitates at the alloy surface.

Wagner's continuum theory of HT oxidation[9,10] and its numerous modifications that have been developed over the years[11] has not provided us with the atomic scale insights necessary for designing new alloys with improved high temperature oxidation resistance. With the advent of multi-principal element alloys (MPEAs) and the need for higher temperature performance there will be renewed interest in this problem since in addition to mechanical properties, oxidation behavior is of primary importance. Exclusive protective scales must form early on in the oxidation process and display good adhesion.

The organization of this paper is as follows. In the next section, we demonstrate the importance of the shape of oxide precipitates within Wagner's formalism using an approach developed by Leblond.[12,13] These results serve to highlight the importance of lateral growth of oxide particles for the formation of an exclusive scale, without the occurrence of internal oxidation. Next, we use a thin-film analogy to develop a kinetic model for the exclusive growth of a protective oxide scale based on oxide/air or metal/oxide interfacial diffusivities and interlayer transport. Hereafter, for brevity, unless required for clarification, we refer to these interfaces as "surfaces" and diffusion occurring within these interfaces as "surface" diffusivity. This model is presumed to be operative during transient oxidation, i.e., prior to the establishment of a steady-state and the development of parabolic kinetics. In this analysis, we first consider the behavior of a model single crystal binary alloy containing a passivating B component and a base metal A, that is incapable of forming a thermally stable oxide. In concert with Wagner's assumption, the oxide particles forming at the surface are assumed to be impenetrable barriers to solid-state mass transport of either the passivating component or oxygen. Following the introduction of the thin film model, we relax the condition connected to the oxidation behavior of the base metal component, A and consider cases involving displacement reactions between the metallic B component and the A-formed oxide. Next, we describe how a dilute alloying component, termed a surfactant, that is capable of segregating to the alloy surface, could serve to increase the nucleation density of passivating oxide islands, which according to the model will enhance the likelihood of forming an exclusive scale. In the Discussion of our results, we present a generic morphology diagram that describes the conditions for exclusive scale formation in terms of the density of passivating oxide particles at the alloy surface and the homologous temperature.

---

[z]E-mail: Karl.Sieradzki@asu.edu

The role of Oxide Precipitate Shape on Exclusive Scale Formation within the Context of Wagner's theory

One of the more interesting modifications of Wagner's theory that has been developed relatively recently involves the use of recursive sequences for parameters entering into the solutions of the diffusion equation.[12–14] Upon iteration, these equations effectively rescale the mole fraction of oxide particles and correspondingly the oxygen diffusivity. This results in significant reductions of the diffusivity and consequential external scale formation. In Wagner's theory, the oxide precipitates are assumed to have a miniscule oxygen diffusivity and so serve as impenetrable barriers to transport. The conditions for exclusive scale formation are $N_O^S/N_B^o \ll 1$ and $D_B/D_O \ll 1$.[1] Here, N_O^S and N_B^o correspond to the surface mole fraction of oxygen or the oxygen solubility in the base metal and the mole fraction of *B*, the scale forming component in the alloy. D_i ($i = O$ or B) is the bulk lattice diffusivity of oxygen or the scale forming component, *B,* in the elemental base metal. These conditions result in simplification of the solutions to the diffusion analysis relating the mole fraction of oxide, N_{BO_ν}, (ν is the stoichiometric coefficient of the oxide) to N_B^o, N_O^s and the diffusivities,[1,11]

$$N_{BO_\nu} = \frac{2\nu}{\pi} N_B^o \frac{N_B^o D_B}{N_O^S D_O}. \qquad [1]$$

The starting point is the use of an effective medium theory (EMT) for how D_O is reduced as a function of the volume fraction, *F*, of BO_ν precipitate particles. Several EMTs have been examined, but the most detailed work is based upon finite element calculations of thermal conductivity yielding,[13]

$$D_O = D_O^o\,(1 - F)^{\chi(W)} \qquad [2]$$

where D_O^o is equal to the oxygen diffusivity in the precipitate-free base metal, $\chi(W) = 1 + 0.44W$, and *W* is equal to the aspect ratio (major axis/minor axis) of the oblate-spheroid shaped precipitates, with their major axis oriented parallel to the surface (i.e., axis of rotational symmetry perpendicular to the surface). The volume fraction of precipitates, *F*, is given by the rule of mixtures,[14]

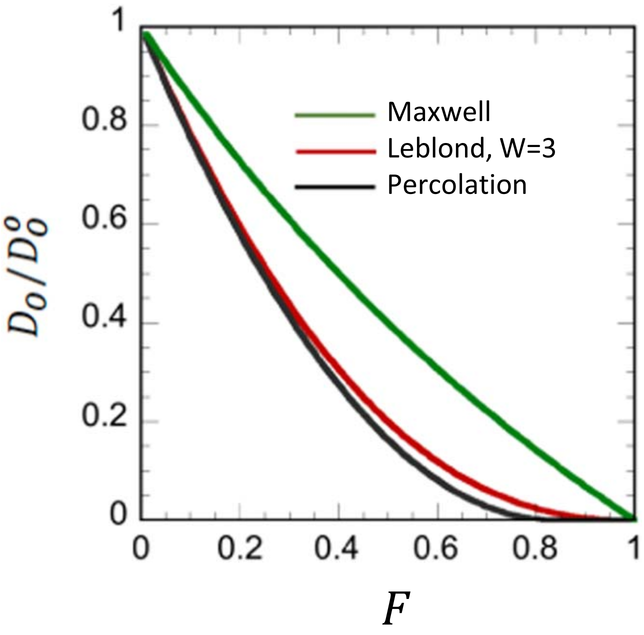

Figure 1. Normalized conductivity as a function of the volume fraction, *F*, of oxide (non-conducting) precipitate.

$$F^n = \frac{\mathfrak{R}}{\mathfrak{R} + \beta^{n-1} D_O^{n-1} - 1} \qquad [3]$$

where $\mathfrak{R}$ is equal to the ratio of the molar volume of the oxide to that of the alloy, $V_{BO_\nu}^M/V_{alloy}^M$, and $\beta = \frac{\pi N_O^S D_O^o}{2\nu (N_B^o)^2 D_B}$. Equation 3 has been written in the form of a recursive sequence where the *n, n*-1, etc, superscripts correspond to successive terms in the sequence. The iterative process starts using Eq. 1 with $F = 0$ and $D_O = D_O^0$ yielding values of $N_{BO_\nu}^0$ and β^0. These are substituted in Eq. 3 to obtain F^1. Then Eq. 2 is used to obtain D_O^1 which is substituted into Eq. 1 to obtain $N_{BO_\nu}^1$ and β^1. The iteration continues until a stable fixed point is reached defined by the condition that $F^n = F^{n-1} = F_{crit}$, the critical volume fraction of the scale forming component. The corresponding critical mole fraction of the scale forming component, $N_{B,\,crit}^o$ is given by $(1/\mathfrak{R})$ F_{crit} and for $N_B^o > N_{B,\,crit}^o$, exclusive scale formation is predicted. Leblond found that he could obtain a result similar to that of Rapp's for Ag-In alloys for a precipitate aspect ratio $W = 3$.[13] Zhao et al., performed a similar analysis,[14] based on an EMT developed by Maxwell,[15] and found that the fixed point was given by,

$$F_{crit} = \frac{2\mathfrak{R}^{1/2}}{6^{1/2} + 2\mathfrak{R}^{1/2}} \qquad [4]$$

For the case of Ag-In alloys, $\mathfrak{R} \cong 2$, so that from Eq. 4, $F_{crit} \cong 0.54$. This discrepancy from Rapp's result of $F_{crit} \cong 0.3$ is connected to various shapes that the precipitate particles can take which is not considered in the EMT used by Zhao et al.[14]

In his first paper on the development of recursive sequences in order to identify the internal/external oxidation transition, Leblond commented on the use of a percolation model, rather than an effective medium theory.[12] We examined this by using an explicit form for the oxygen conductivity based on percolation theory,[16]

$$D_O = D_O^0 \left(\frac{1 - F^* - F}{1 - F^*} \right)^t = D_O^0 \left(\frac{0.84 - F}{0.84} \right)^2, \qquad [5]$$

where, F^* is the percolation threshold of the conducting phase. This is equal to about 0.16 for the case of continuum percolation of a random close-packed structure[17,18] and *t,* the conductivity exponent in three dimensions is equal to 2.[19] Figure 1 shows a plot of D_O/D_O^0 versus *F* which is qualitatively similar to the Leblond and Maxwell effective medium models with the important distinction that $D_O/D_O^0 = 0$ for $F \geqslant 0.84$.

The expression for D_O in Eq. 5 is substituted into Eq. 3 to obtain the recursive sequence,

$$F^n = \frac{\mathfrak{R}}{\mathfrak{R} + \beta^{n-1} \left(\frac{0.84 - F^{n-1}}{0.84} \right)^2 - 1} \qquad [6]$$

As shown in Fig. 2a, we solved this recursion graphically for Ag-In alloys ($\mathfrak{R} \cong 2$). The solution to the recursion relation for the critical volume fraction of oxide particles is $\cong 0.30$, but the similarity to Rapp's result may simply be a coincidence, since Eq. 5 does not consider the shape of the oxide particles.

In order to explore this in more detail, we solved the recursive sequences for the percolation model and both the finite element derived EMT developed by Leblond[13] and Maxwell's EMT used by Zhao et al.[14] as a function of $V_{BO_\nu}^M/V_{alloy}^M$. Figure 2b shows that both the percolation and Leblond's model for $W = 3$ are in good agreement, however the range of $F_{\rm crit}$ values attainable as a function of $V_{BO_\nu}^M/V_{alloy}^M$ for all three models is limited. Figure 3, developed

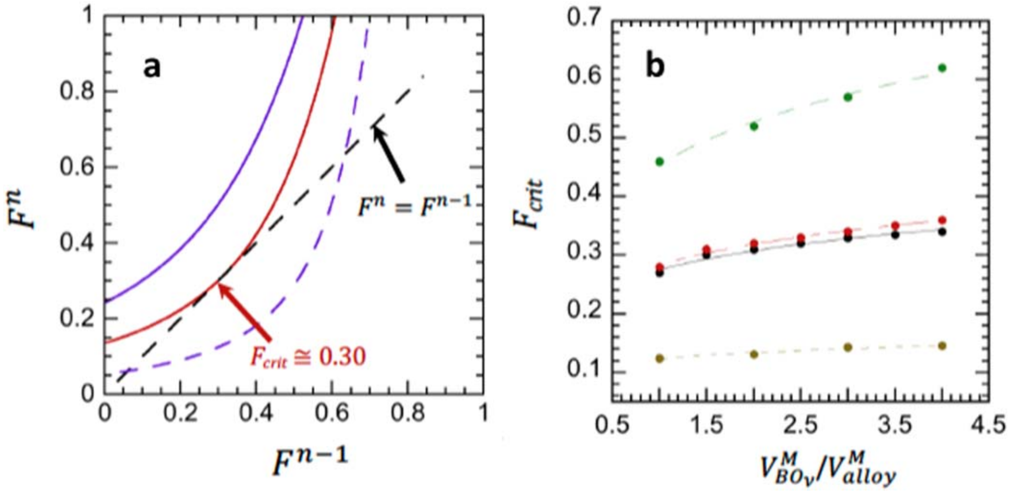

Figure 2. Results of a graphical solution to the recursion relations. a. Continuum percolation model showing that $F_{crit} \cong 0.30$. The critical value of β in Eq. 6 is 13.3. The formation of an exclusive external scale is predicted for β less than the critical value and internal oxidation is predicted for β greater than the critical value. For example, the solid blue line corresponds to $\beta = 7$ and the dashed blue line corresponds to $\beta = 35$. b. Solutions to the recursive sequences for the percolation model (black), Leblond's EMT (W = 3 red: W = 10 brown) and Maxwell's EMT (green) as a function of $V^M_{BO_\nu}/V^M_{alloy}$. Dashed lines are guides to the eye.

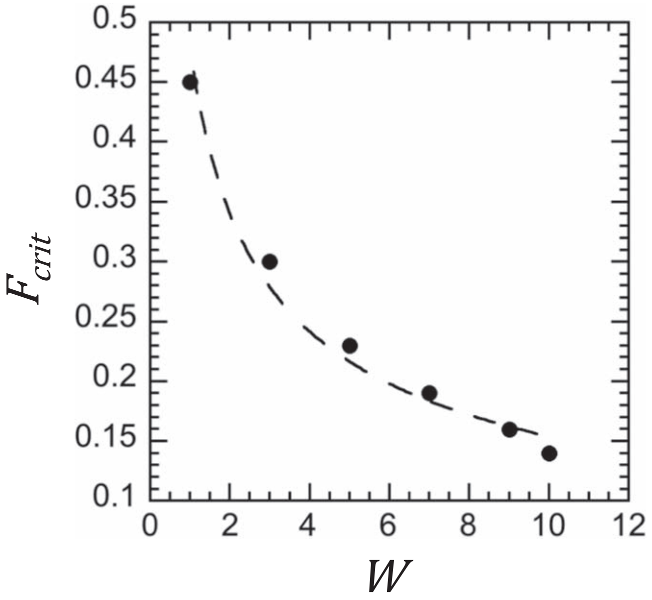

Figure 3. Leblond's EMT prediction for the critical volume fraction of oxide precipitates as a function of the particle aspect ratio *W*. The dashed line is a guide to the eye.

using Leblond's EMT for $V^M_{BO_\nu}/V^M_{alloy} = 2$, is an example of how the shape of the oxide precipitates affect F_{crit}. There is clearly a stronger effect of aspect ratio, *W*, than that observed in Fig. 2b for the molar volume ratio. Our analyses of these results suggest that without consideration of precipitate shape and orientation, both of which relate to the importance of lateral growth, the correct physics controlling the transition cannot be understood within the context of any theory. While there has been some attention to characterizing oxide precipitate size distributions and morphology using carbon replica/TEM techniques,[20] to date, these characterizations are not sufficiently quantitative for verifying the use of the recursive approach in determining the conditions required for exclusive scale formation. We suggest that given these issues, it seems worthwhile to explore other models of exclusive scale formation in the HT oxidation of alloys.

Thin Film Growth Analogy

As discussed in the Introduction, if exclusive protective scales are to form, this must occur early on in the HT oxidation process. To the best of our knowledge, all HT oxidation experimental work employ samples with an initial condition of air-formed surface oxides as virtually all elemental metals "oxidize" to some extent (even if only a chemisorbed monolayer) in air at ambient temperature. These air-formed oxides very quickly give way to the HT oxide growth process described below. Nevertheless, it is instructive, in a general sense, to discuss how these ambient temperature air-formed oxides form in elemental transition metals and aluminum. We note that this has been rather extensively explored in the past 20 years using a variety of experimental approaches and first-principles based calculations owing to the interest in oxidation catalysts.[21–31] Here, we summarize the most general features of these investigations which pertain to the transition from an initial chemisorbed phase to a sub-surface oxide phase.

The important aspect of the chemisorption of dioxygen is the development of full coverage, low-density, adsorbed surface phases. Full coverage, low-density means that, for example, in the case of a FCC (111) surface, every *nth* three-fold hollow normal FCC site on the surface is occupied. Thus while the coverage, as measured with respect to surface occupation, θ is only $1/n$, the surface is uniformly covered with this low-density adsorbed phase. With increasing quantities of oxygen adsorption, the density of these full-coverage phases increase, as does the magnitude of repulsive interactions in the electronegative oxygen adlayer.[21,25] Eventually, at a critical value of θ, it becomes thermodynamically favorable for oxygen to be incorporated into sub-surface interstitial sites.[22] This incorporation is effectively the nucleation of sub-oxides with structural units that may be already indicative of thermodynamically stable BO_ν.[31] At least in part, since sub-surface oxygen incorporation involves a lattice expansion, the critical value of θ at which this occurs is dependent on the elastic properties of the metal.[21] We expect that once oxygen is incorporated sub-surface, that thermodynamically stable isolated oxide nuclei form quickly. Thus, we can expect that the air-formed film may already contain BO_ν nuclei which could serve as initiation sites of transient HT oxidation.

In what follows we adapt the model of thin film growth kinetics in Tersoff et al.[32] to the problem of exclusive scale formation. While there have been several modifications to these general concepts,[33–35] the clearest explanation of the general ideas is made in.[32] For the simplest case, we consider a single crystal alloy containing a passivating *B* component and a base metal *A*, that is incapable of forming a thermally stable oxide. The flux of molecular oxygen to the alloy surface, J_{O_2}, is controlled by the external oxygen pressure and from kinetic theory is $P_{O_2}/\sqrt{2\pi\ m_{O_2}k_BT}$, where m_{O_2} is the mass of the oxygen molecule. The flux of the passivating component to the surface, J_B scales as $(D_B/t)^{1/2}$. For oxygen and *B* atoms arriving at or already present at either the alloy/BO$_\nu$ interface and/or P_{O_2}/BO$_\nu$ interface locations not occupied by BO$_\nu$ islands, there are two possible outcomes. Either new oxide islands will nucleate between previously existing ones and/or the concerted surface diffusion of both components results in attachment at the steps of pre-existing islands, i.e., growth by a step-flow mechanism (Fig. S1).

Figure 4 shows a two-dimension cross-section of a vicinal surface that we use to discuss the portion of J_B arriving at pre-existing oxide island locations. This problem is similar to that of heteroepitaxial deposition except that the interfacial diffusion processes responsible for lateral growth may occur at a buried alloy/BO$_\nu$ interface and/or at a P_{O_2}/BO$_\nu$ interface. There are three competing length scales shown. The mis-cut defines a length scale, L_s, in the problem corresponding to the physical extent of a terrace on a vicinal or vicinal-like surface.[32] If the surface has been mechanically or (electro) chemically polished, the surface could contain steps many monolayers in height, but an average L_s could be defined by appropriate characterization with an atomic force microscope or similar device. A second length scale is $L_\alpha = 2a/\alpha$, where *a* is the hopping distance and $\alpha = \exp(-\Delta E_{ES}/k_BT)$, corresponds to the probability that an atom will cross over the oxide step edge, which behaves as a diffusion barrier. In heteroepitaxial thin film growth, the Ehrlich-Schwoebel (ES) barrier can result from a loss of neighbors for an atom at a descending step as well as a change in neighbor identity.[36,37] ΔE_{ES} is the amount by which the activation energy for crossing the barrier exceeds that for surface diffusional hopping. Heuristically, one can consider L_α to correspond to the number of times the diffuser visits the barrier prior to crossing, multiplied by the size of the island. A third length scale in the figure, $L_n = (4a^2D_s^i/J_B)^{1/6}$, (where D_s^i is the surface diffusivity, $i = B$ and/or *O*) corresponds to about half the distance between islands or half the average island size.[32] If an island of radius *R* is larger than a critical size, R_c, nucleation of a new layer will occur prior to the diffuser surmounting the ES barrier resulting in vertical (i.e., 3D) island growth. This means that the interlayer transport of atoms arriving at these surfaces must be rapid, otherwise, nucleation of islands occurs on the uncompleted growing monolayers of BO$_\nu$ For growth occurring at the P_{O_2}/BO$_\nu$ interface, D_s^i will correspond to the surface diffusivity of dioxygen molecules and/or oxygen atoms. For the buried interface, while there may be no loss of neighbors for a *B*-atom attempting to cross the step edge, surface defects (e.g., dislocations, vacancies) in addition to thermodynamic factors such as neighbor identities may still impose such a barrier.[38] If the ES barrier and its associated length scale, L_α is small enough in comparison to R_c, lateral growth by island coalescence will take place (i.e., layer-by-layer growth), otherwise, 3D island growth will occur. These length scales were used by Tersoff to develop a criterion for lateral island growth,[32]

$$\Delta E_{ES} < (k_BT/6)\ln(D_s^i/J_Ba^4) \tag{7}$$

Note that the right-hand side (RHS) of Eq. 7 is maximized for large D_s^i and small J_B. In the composition range $(0.05 < N_B^0 < 0.25)$ and over the time scales of interest (1–60 s), J_B will only change by a factor of ∼10.

We consider the HT oxidation behavior of two exemplary alloys, Ag$_{0.85}$In$_{0.15}$ and Fe$_{0.80}$Cr$_{0.20}$ at $P_{O_2} \approx 10^5$ Pa for the case of a buried interface, at temperatures of 823 K and 1273 K respectively. At the indicated temperatures the lattice diffusivities, D_{In} and D_{Cr} are available from existing literature.[10] Here $J_B \approx 0.05N_B^o n_A/V_{alloy}^M(D_B/\pi t)^{1/2}$, where n_A is Avogadro's number. For each of these alloys, J_B is evaluated at $t = 1$ s and D_s^i, while unknown, is taken to be of order 10^{-6} cm^{2}s^{-1}, in order to maximize the RHS of the equation. In the case of Ag$_{0.85}$In$_{0.15}$ the RHS of Eq. 7 is 0.25 eV and in the case of Fe$_{0.80}$Cr$_{0.20}$ it is 0.40 eV. This analysis predicts that for ΔE_{ES} less than the indicated values, growth of exclusive scales should occur. More generally, if $\Delta E_{ES} < k_BT$, then $L_\alpha < L_n$ and lateral growth of the oxide and exclusive scale formation will occur. At a temperature of ∼1250 K this corresponds to ∼0.10 eV. The appropriate E_{ES} values for these systems are currently unknown, however, in the case of thin film growth of metals, ES barriers are in the range of $0.02 - 0.50$ eV.[39–41] There are also a few reports in the literature discussing the magnitude of these barriers for growth on oxide surfaces which are in the same range of values.[42–45]

As illustrated in Fig. 5, if the ES barrier is too large, 3D cluster growth occurs. Nevertheless, if the space between the islands is small enough, corresponding to a high particle density, then the 1st layer of oxide islands may still be able to close up, forming a protective scale prior to measurable internal oxidation. Monte Carlo simulations and continuum calculations[46,47] for such cluster growth

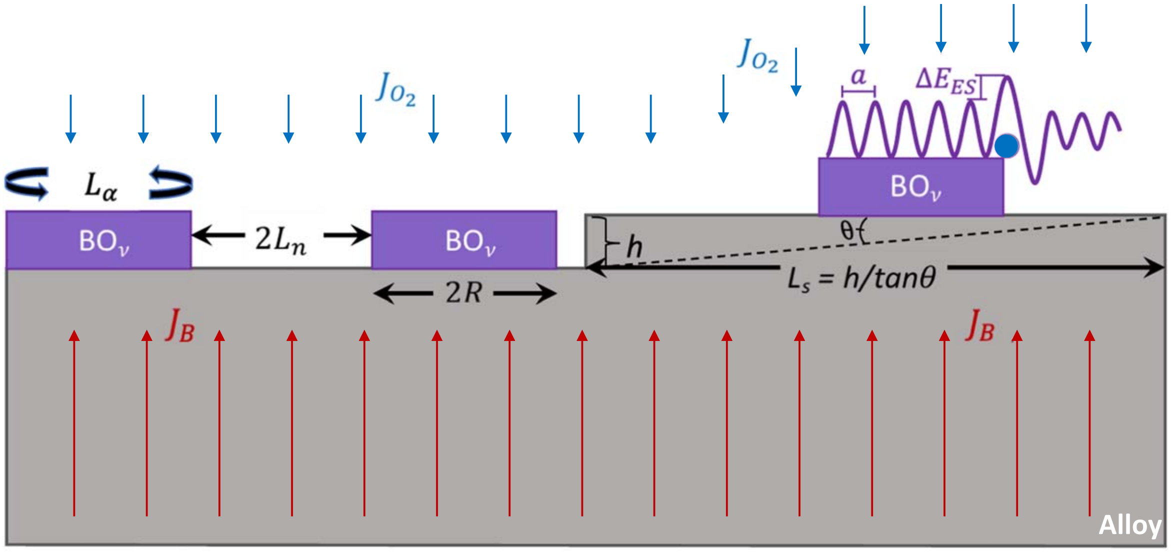

Figure 4. Length scales defining the competition between layer-by-layer resulting in island coalescence of oxide particles and 3D island or cluster growth. Cluster formation at the O$_2$/alloy interface involves interface diffusion of oxygen and/or *B*.

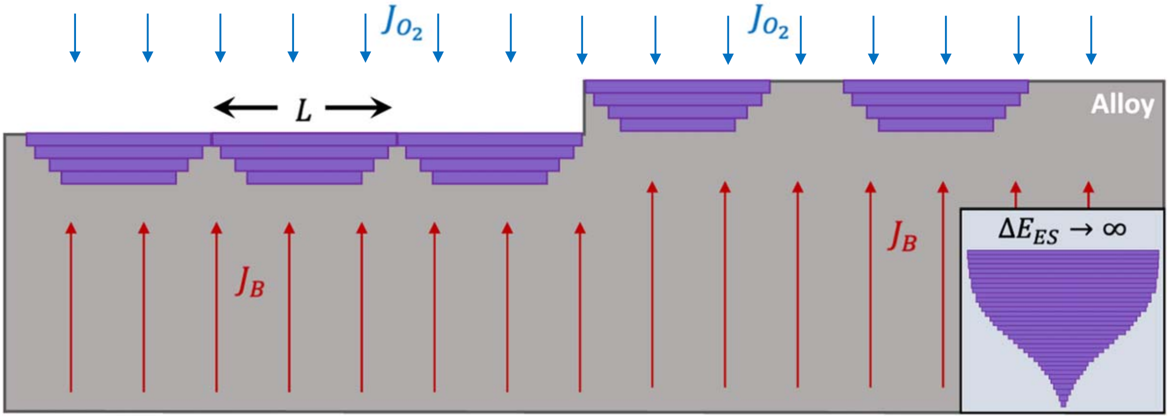

Figure 5. "Wedding-cake" shaped 3D islands forming at a buried alloy/oxide interface. If the island density is large enough, they can coalesce as shown across the left-most terrace, forming a portion of the protective oxide scale. The inset shows the asymptotic shape of the clusters in the limit of an infinitely large ES barrier.

in thin film deposition have shown that the clusters can evolve into the "wedding cake"- or pear-shaped morphologies observed in HT oxidation of a $NiAl_{0.08}Cr_{0.08}$ alloy[14] and an equimolar CoCrFeNi alloy.[6] The shape function describing the asymptotic cluster boundary, in the limit of an infinitely large ES barrier, is $\Phi(x) = 1 - C[1 + erf\,(x/\sqrt{2}\,)]$,[46] where C is an integration constant effectively defining the extent of the island base. Importantly, if the islands grow too large in the vertical direction prior to coalescence, then bulk diffusion transport to the island bases becomes sterically hindered which could significantly delay lateral island growth resulting in internal oxidation. These wedding-cake shaped oxide islands could eventually evolve into 1D wire-like structures that would serve to define the protective scale morphology at length scales larger than the thickness of the scale defined by the base of the wires. A qualitative picture of the formation of HT protective Al_2O_3 scales similar to Fig. 5 has been previously discussed, but not within the context of thin-film growth.[48]

Based on the analysis of the thin-film model presented above, we now consider the effect of relaxing the restriction on the model system related to the stability of the oxide of the base metal component A. For example, for Fe-Cr, Ni-Cr and Co-Cr alloys, the base metals can form thermally stable oxides at relevant temperatures in HT oxidation. In this scenario, Cr_2O_3 nuclei could form either by a general displacement reaction, $Cr + xAO_\nu = CrO_{x\nu} + xA$ or direct reaction with oxygen. In either case, crystal steps/kinks which are the most reactive sites on the surface would likely serve as locations for the formation of Cr_2O_3 nuclei that could undergo lateral growth by a step-flow mechanism. In the case of Cr_2O_3 islands forming on terraces by direct reaction with oxygen, the interlayer transport processes described above are still expected to be operative. However, the surface would no longer serve as an "instantaneous" sink for B-atoms so that the time required for the formation of a continuous BO_ν scale could significantly increase from seconds to many minutes.

Surfactant Effects

In what follows, we briefly describe approaches for increasing the surface nucleation density of oxides by the use of what may be termed a "surfactant."[39,49–52] Here we use this term to mean a dilute alloy component capable of segregating to the alloy surface and step edges. The driving force for segregation of this component is a lowering of the interfacial/step energy and/or a high affinity for oxygen. Figure 6 illustrates the possible atomic-scale mechanisms of such a surfactant.[49,53] One involves finessing the ES barrier associated with interlayer transport by an exchange process that could also involve a displacement reaction. In direct exchange (indicated by 1 in Fig. 6), a B-atom (indicated in red color) exchanges places with the surfactant component indicated in gold color. This could have the beneficial effect of lowering the elastic energy associated with the formation of a BO_ν phase since the volume dilation may be significantly reduced. A second process (indicated by 2 in Fig. 6), involves a direct reduction of the ES barrier if the surfactant segregates to the edge of an existing island. In this case, the B component exchanges its position with the surfactant atom leaving the latter attached to island edge. Each of these mechanisms could enhance the formation an exclusive scale under N_B^o, P_{O_2} and T conditions for which this would not otherwise occur. In addition to these mechanisms, such a surfactant could also increase the nucleation density by lowering step edge energies (indicated by 3 in Fig. 6) and so the activation energy for nucleation.

Discussion

The ES barrier length scale, L_α, decreases exponentially with increasing temperature. L_n is a function of D_s^i and J_B and both of these quantities relate to thermally activated hopping. Generally, since the activation energy for bulk diffusion, E_B, is larger than that for surface diffusion, E_S, the quantity $(D_s^i\,/J_B)$ will scale as $exp\ (E_B - E_S)$ for which $E_B - E_S > 0$, indicating that L_n will also decrease with increasing temperature. Island coalescence will occur prior to 3D growth if $L_\alpha < L_n$. The temperature at which this occurs, T_{IC}, is defined by the condition, $L_n \approx R_c$. Figure S2 (supplementary data stacks.iop.org/JES/169/061501/mmedia) shows results for the temperature dependence of L_α and L_n for realistic parameter values. As a result of the exponential decrease of L_α with temperature, unless BO_ν vaporization processes intercede, there will always be a high enough temperature for which $L_\alpha < L_n$ so that layer-by layer growth will occur either by island coalescence or step flow ($L_s < L_n$). As shown in Fig. 7, these considerations allow for the construction of a generic morphology diagram for exclusive scale formation for an A_pB_{1-p} alloy for p in the range of 0.80–0.95. The figure shows three general regimes for exclusive scale formation. One occurs in the region of high enough oxide island nucleation density for which little lateral diffusion is required for the oxide islands to coalesce (blue). A second regime occurs when $L_\alpha < L_n$ and requires significant lateral growth for island coalescence (red). A third region occurs at high enough temperature for which $L_n \approx L_s < L_\alpha$ (grey/gold).

We have some suggestions for experimental validation of the general concepts described in the proposed thin film model. Single-crystal alloy samples such as Ag-In or Fe-Cr could be heated to the temperature of interest in a reducing or non-oxidizing atmosphere. Afterwards, the samples would be exposed to the oxidizing atmosphere for very short periods of time. Alternatively, samples could be configured such that the time to reach the prescribed oxidation

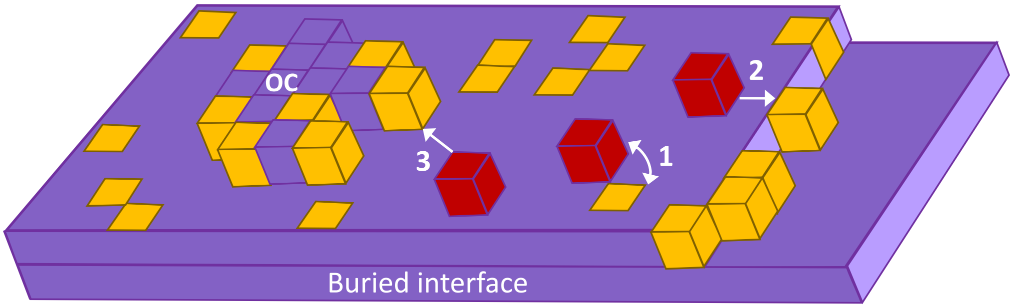

Figure 6. Illustration of how a suitable surfactant could affect both the lateral growth and the nucleation density of BO_ν oxide (violet color) clusters for the case for the case of a buried interface. The B passive film forming metallic atoms are in red color and the surfactant atoms are in gold color. Surfactant atoms are located within the terrace (of the oxide), and at step-edge positions. OC is an oxide island cluster with surfactant atoms located at the island perimeter. The numbers 1, 2, 3 and corresponding arrows, show examples of surfactant-mediated exchange processes described in the text.

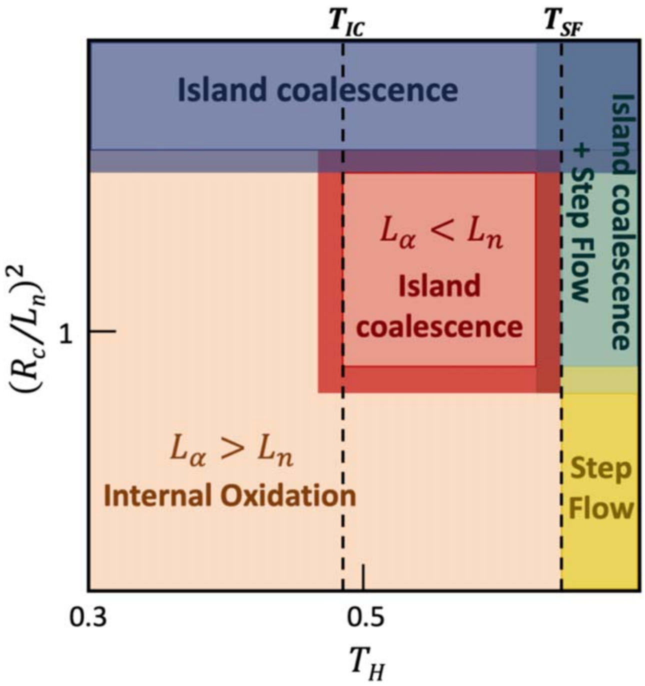

Figure 7. Generic morphology diagram for exclusive scale formation (ESF). The *x*-axis is the homologous temperature of the alloy, T_H, and the *y*-axis corresponds to the dimensionless density, $(R_c/L_n)^2$, of oxide islands forming at the alloy surface. ESF by layer-by-layer growth resulting in island coalescence can occur when $(R_c/L_n)^2 > 1$ and $T > T_{IC}$ where T_{IC} corresponds to the temperature at which $L_\alpha < L_n$ (Supplementary Material). At a high enough temperature, $L_\alpha < L_n$ and $< L_s$, so island coalescence and/or step flow growth is predicted resulting in ESF. Below about $T_H/3$, lattice diffusion is limited. At a high enough nucleation density 3D islands can coalesce as shown in Fig. 5. T_{SF} corresponds to temperatures for which both island coalescence and step-flow growth can occur. Boundary lines are not meant to indicate a sharp transition between regimes and overlapping colors correspond to surfactant effects.

temperature in the oxidizing environment is short (~1 min) as was done by Chattopadhyay and Wood.[2] Characterization would involve FIB sectioning and SEM examination of the cross-section. Alternatively, FIB machined STEM samples could be taken from the alloy surface and characterized. We note that the work of Yu et al. already provides some proof of concept for such experiments.[6] Ehrlich-Schwoebel barriers could be calculated using first-principles approaches and model predictions could be compared to the experimental characterization results. Additional experiments could be conducted with a polycrystal of the same alloy in order to elucidate grain boundary effects.

While we find that the thin-film growth model described above is, in principle, able to make quantitative predictions for the formation of exclusive scales, various parameters such as the relevant ES barriers and the interfacial diffusivities are currently unknown. An improved understanding of exclusive scale formation in HT oxidation centers around several important issues occurring very early in HT oxidation, that today, are amenable to experimental characterization and first-principles based calculations.

One issue is related to the size, shape and density of the oxide particles forming at the surface. It seems that Rapp's identification of a "critical" volume fraction of oxide for the Ag-In system of ≈ 0.3 is a number almost universally used as a scale forming criterion for many alloys that have been studied. Yet clearly, based on our analysis, the shape of the oxide particles seems crucial for establishment of a critical volume fraction of oxide precipitates, which depends on surface and bulk transport in the alloy as well as the nucleation and growth of oxide particles. A consequence of Wagner's original model is that the oxide particles forming in the inner oxidation zone are homogeneously distributed within that zone. Yet, in order for exclusive scale formation to occur, one would expect that a much higher density of particles actually forms very close to, or at the surface with a steep gradient of the oxide volume fraction going into the bulk of the alloy [see Fig. 6.25 in Ref. 11]. Additionally, an important related question is, how does the grain size of the oxide forming the external scale compare to the thickness of the scale? This type of characterization would provide us with information on important details of the oxide growth process.

A second issue connects to surface and/or interfacial diffusivities and the magnitude of ES barriers. There has been some determination of these barriers in thin film deposition using scanning tunneling microscopy. This was done by examining the formation and relative populations of 2nd and 3rd layers of Ag clusters on previously grown and well characterized primary Ag islands on Pt(111).[41] An Avrami-like analysis was used to determine a critical island size, R_c, for 3D cluster growth. This data was used in conjunction with equations developed in[32] from which the barrier was calculated. It is important to note that there are two different kinetic mechanisms for navigating the barrier. One involves step-edge crossing as illustrated in Fig. 4. The other involves direct incorporation through a terrace into the oxide particle which finesses step-edge crossing.[21,49] While these parameters may be accessible via scanning probe or low energy electron microscopy, first principles approaches may yield the most reliable values and will also be able to inform us on the details of the mechanism for overcoming the barrier. STM has also been used to investigate the growth of oxides on Ni- Cr(100) alloy surfaces between 300 °C–500 °C.[54–56] Modeling suggested that in this temperature range, oxygen surface diffusion controls lateral growth and coalescence of NiO islands.[54]

The possible beneficial effects of surfactants, which is a dilute alloying effect, may be related to some of the so-called "reactive element" effects, which have received considerable attention in the

HT oxidation literature.[57–59] There have been numerous mechanisms proposed for these effects and our discussion of surfactants is another way of thinking about how dilute alloying components could contribute to the process of exclusive protective scale formation. More recently, the general qualitative concepts of increased nucleation density and lateral oxide growth have been discussed with respect to the θ–to α–Al_2O_3 phase transformation,[60] but the detailed atomic scale processes remain an open issue that may benefit from our description of surfactant effects. There are of course well-known effects of some of these additives that our analysis does not directly address, for example, the gettering of deleterious impurities such as sulfur which can result in substantially improved scale adhesion.

Conclusions

A thin-film growth analogy has the potential to provide some insights for an understanding of the atomic-scale processes involved in exclusive scale formation in the HT oxidation of alloys. The unknown parameters required to test the usefulness of this approach includes the surface/interfacial diffusivities of oxygen species as well as that of the scale forming component and the magnitude of ES barriers. These values should be amenable to first-principles-based calculations. Additionally, suitably designed scanning probe experiments may be able to provide experimental information regarding surface diffusivities as well as the magnitude of the ES barriers. Even lacking these results, our analysis shows that for a large enough nucleation density of oxide particles exclusive scales should form.

The key unknown parameters in the recursive sequence analysis of Wagner's formulation are the shape, size and orientation of the oxide particles forming close to the surface. A statistical characterization of these parameters would make it possible to develop a corresponding effective medium or percolation model that could be used to test this approach.

There remains a considerable amount of research to be performed using modern electron microscopy techniques characterizing exclusive scales both during the formation process as well as following its completion. We suggest that such characterization be first performed on elemental metals or binary alloy systems under intensive thermodynamic conditions and at compositions known to result in exclusive scales.

Acknowledgments

The authors thank D.J. Young and P. Reinke for examining earlier versions of this manuscript and for providing helpful suggestions and comments. The authors acknowledge support from the Office of Naval Research, Multidisciplinary University Research Initiative program, "From Percolation to Passivation (P2P): Multiscale Prediction and Interrogation of Surface and Oxidation Phenomena in Multi-Principal Element Alloys" under Grant Number N00014-20-1-2368.

ORCID

William H. Blades https://orcid.org/0000-0002-0665-7981
Karl Sieradzki https://orcid.org/0000-0002-4789-3956

References

1. R. A. Rapp, "Kinetics, microstructures and mechanism of internal oxidation; its effect and prevention in high temperature alloy oxidation." *Corrosion*, **21**, 82 (1965).
2. B. Chattopadhyay and G. C. Wood, "The transient oxidation of alloys." *Oxid. Met.*, **2**, 373 (1970).
3. G. Zhou, L. Luo, L. Li, J. Ciston, E. A. Stach, and J. C. Yang, "Step-edge-induced oxide growth during the oxidation of Cu surfaces." *Phys. Rev. Lett.*, **109**, 235502 (2012).
4. Q. Zhu, W. A. Saidi, and J. C. Yang, "Enhanced mass transfer in the step edge induced oxidation on Cu(100) surface." *J. Phys. Chem. C*, **121**, 11251 (2017).
5. L. Luo, L. Zou, D. K. Schrieber, M. J. Olszta, D. R. Baer, S. M. Bruemmer, G. Zhou, and C.-M. Wang, "*In situ* atomic scale visualization of surface kinetics driven dynamics of oxide growth on a Ni-Cr surface." *Chem. Commun.*, **52**, 3300 (2016).
6. X.-X. Yu, M. A. Taylor, J. H. Perepezko, and L. D. Marks, "Competition between thermodynamics, kinetics and growth mode in the early-stage oxidation of an equimolar CoCrFeNi alloy." *Acta Mater.*, **196**, 651 (2020).
7. K. Wagner, S. R. Brankovic, N. Dimitrov, and K. Sieradzki, "Dealloying below the critical potential." *J. Electrochem. Soc.*, **144**, 3545 (1997).
8. R. A. Rapp, "The transition from internal to external oxidation and the formation of interruption bands in silver-indium alloys." *Acta Metall.*, **9**, 730 (1961).
9. C. Wagner, "Theoretical analysis of the diffusion processes determining the oxidation rate of alloys." *J. Electrochem. Soc.*, **99**, 369 (1952).
10. C. Wagner, "Oxidation of alloys involving noble metals." *J. Electrochem. Soc.*, **103**, 571 (1956).
11. D. J. Young, *High Temperature Oxidation and Corrosion of Metals* (Elsevier, Amsterdam) 2nd ed. (2016).
12. J.-P. Leblond, "A note on a nonlinear version of Wagner's classical model of internal oxidation." *Oxid. Met.*, **75**, 93 (2011).
13. J.-P. Leblond, M. Pignol, and D. Huin, "Predicting the transition from internal to external oxidation of alloys." *C.R. Mecanique*, **341**, 314 (2013).
14. W. Zhao, Y. Kang, J. M. A. Orozco, and B. Gleeson, "Quantitative approach for determining the critical volume fraction for the transition from internal to external oxidation." *Oxid. Met.*, **83**, 187 (2015).
15. J. C. Maxwell, *Treatise on Electricity and Magnetism* (Clarendon, Oxford) (1904).
16. T. R. Ferguson and M. Z. Bazant, "Nonequilibrium thermodynamics of porous electrodes." *J. Electrochem. Soc.*, **159**, A1967 (2012).
17. R. Zallen, *The Physics of Amorphous Solids* (Wiley, New York, NY) (1983).
18. C.-W. Nan, "Physics of inhomogeneous inorganic materials." *Prog. Mater Sci.*, **37**, 1 (1993).
19. D. Stauffer and A. Aharony, *Introduction to Percolation Theory* (Taylor and Francis, London) 2nd ed. (1991).
20. P. Bolsaitis and M. Kahlweit, "The internal oxidation of Cu-Si Alloys." *Acta Metall.*, **15**, 765 (1967).
21. M. Todorova, W. X. Li, M. V. Ganguglia-Pirovano, C. Stampfl, and M. Scheffler, "Role of subsurface oxygen in oxide formation at transition metal surfaces." *Phys. Rev. Lett.*, **89**, 096103 (2002).
22. C. I. Carlisle, T. Fujimoto, W. S. Sim, and D. A. King, "Atomic imaging of the transition between oxygen chemisorption and oxide film growth on Ag{111}." *Surf. Sci.*, **470**, 15 (2000).
23. C. Stampfl, M. V. Ganduglia-Pirovano, K. Reuter, and M. Scheffler, "Catalysis and corrosion: the theoretical surface-science context." *Surf. Sci.*, **500**, 368 (2002).
24. K. Reuter, C. Stampfl, M. V. Ganduglia-Pirovano, and M. Scheffler, "Atomistic description of oxide formation on metal surfaces: the example of ruthenium." *Chem. Phys. Lett.*, **352**, 311 (2002).
25. C. Stampfl, A. Soon, S. Piccinin, H. Shi, and H. Zhang, "Bridging the temperature and pressure gaps: close-packed transition metal surfaces in an oxygen environment." *J. Phys. Condens. Matter*, **20**, 184021 (2008).
26. I. Köhler et al., "High-coverage oxygen structures on Rh(111): adsorbate repulsionand site preference is not enough." *Phys. Rev. Lett.*, **93**, 266103 (2004).
27. P. Winkler, J. Zeininger, Y. Suchorski, M. Stoger-Pollach, P. Zeller, M. Amati, L. Gregoratti, and G. Rupprechter, "How the anisotropy of surface oxide formation influences the transient activity of a surface reaction." *Nat. Commun.*, **12**, 69 (2021).
28. G. Ketteler, D. F. Ogletree, H. Bluhm, H. Liu, E. L. D. Hebenstreit, and M. Salmeron, "In Situ spectroscopic study of the oxidation and reduction of Pd (111)." *J. Am. Chem. Soc.*, **127**, 18269 (2005).
29. H. Zhang, A. Soon, B. Delley, and C. Stampfl, "Stability, structure, and electronic properties of chemisorbed oxygen and thin surface oxides on Ir(111)." *Phys. Rev. B*, **78**, 045436 (2008).
30. W.-X. Li, C. Stampfl, and M. Scheffler, "Oxygen adsorption on Ag (111), a density-functional theory investigation." *Phys. Rev. B*, **65**, 075407 (2002).
31. A. Kiejna and B. I. Lundqvist, "First-principles study of surface and subsurface O structures at Al(111)." *Phys. Rev. B*, **63**, 085405 (2001).
32. J. Tersoff, A. W. Denier van der Gon, and R. M. Tromp, "Critical island size for layer-by-layer growth." *Phys. Rev. Lett.*, **72**, 266 (1994).
33. J. Rottler and P. Mass, "Second layer nucleation in thin film growth." *Phys. Rev. Lett.*, **83**, 3490 (1999).
34. J. Krug, P. Politi, and T. Michely, "Island nucleation in the presence of step edge barriers: Theory and applications." *Phys. Rev. B*, **61**, 14037 (2000).
35. J. Krug, "Scaling regimes for second layer nucleation." *Eur. Phys. J. B*, **18**, 713 (2000).
36. G. Ehrlich and F. G. Hudda, "Atomic view of surface self-diffusion: tungsten on tungsten." *J. Chem. Phys.*, **44**, 1039 (1966).
37. R. L. Schwoebel, "Step motion on crystal surfaces." *II, J. Appl. Phys.*, **40**, 614 (1969).
38. P. Politi, G. Grenet, A. Marty, A. Ponchet, and J. Villain, "Instabilities in crystal growth by atomic or molecular beams." *Phys. Rep.*, **324**, 271 (2000).
39. J. Camarero et al., "Epitaxial growth of metals with high ehrlich-schwoebel barriers and the effect of surfactants." *Appl. Phys. A*, **69**, 533 (1999).
40. H. Ibach, *Physics of Surfaces and Interfaces* (Springer, Berlin) (2006).
41. K. Bromann, H. Brune, H. Roder, and K. Kern, "Interlayer mass transport in homoepitaxial and heteroepitaxial metal growth." *Phys. Rev. Lett.*, **75**, 677 (1995).

42. A. G. Gianfrancesco, A. Tselev, A. P. Baddorf, S. V. Kalinin, and R. K. Vasudevan, “The ehrlich–schwoebel barrier on an oxide surface: a combined Monte-Carlo and *in situ* scanning tunneling microscopy approach.” *Nanotechnology*, **26**, 455705 (2015).
43. D. E. Ashenford, F. Long, W. E. Hagston, B. Lunn, and A. Matthews, “Experimental and theoretical studies of the low-temperature growth of chromia and alumina.” *Surf. Coat. Tech.*, **116-119**, 699 (1999).
44. F. Sedona, M. Sambi, L. Artijlia, G. A. Rizzi, A. Vittadini, A. Fortunelli, and G. Granozzi, “Mobility of Au on TiOx substrates with different stoichiometry and defectivity.” *J. Phys. Chem. C*, **112**, 3187 (2008).
45. V. Gervilla, G. A. Almyras, F. Thunström, J. E. Greene, and K. Sarakinos, “Dynamics of 3D-island growth on weakly-interacting substrates.” *Appl. Surf. Sci.*, **488**, 383 (2019).
46. J. Krug and P. Kuhn, “Second layer nucleation and the shape of wedding cakes.” *Atomistic Aspects of Epitaxial Growth*, ed. M. Kotrla, N. I. Papanicolaou, D. D. Vvedensky, and L. T. Wille (Nato Science Series) 145 (2002).
47. J. Krug, “On the shape of wedding cakes.” *J. Stat. Phys.*, **87**, 505 (1997).
48. F. H. Stott, “The protective action of oxide scales in gaseous environments at high temperature.” *Rep. Prog. Phys.*, **50**, 861 (1987).
49. Z. Zhang and M. G. Legally, “Atomic-scale mechanisms for surfactant-mediated layer-by-layer growth in homoepitaxy.” *Phys. Rev. Lett.*, **72**, 693 (1994).
50. H. A. van der Vegt, H. M. van Pinxteren, M. Lohmeier, E. Vlieg, and J. M. C. Thornton, “Surfactant-induced layer-by-layer growth of Ag on Ag(111).” *Phys. Rev. Lett.*, **68**, 3335 (1992).
51. K. Sieradzki, S. R. Brankovic, and N. Dimitrov, “Electrochemical defect-mediated thin-film growth.” *Science*, **284**, 138 (1999).
52. S. R. Brankovic, N. Dimitrov, and K. Sieradzki, “Surfactant mediated electrochemical deposition of Ag on Au(111).” *Electrochem Solid St. Lett.*, **2**, 443 (1999).
53. G. Ehrich, “Atomic events at lattice steps and clusters: a direct view of crystal growth processes.” *Surf. Sci.*, **331-333**, 865 (1995).
54. R. Ramanathan, G. Ramalingam, J. H. Perepezko, P. Reinke, and P. W. Voorhees, “Evolution of NiO island size distributions during the oxidation of a Ni–5Cr Alloy: experiment and modeling.” *ACS Appl. Mater. Interfaces*, **10**, 9136 (2018).
55. W. H. Blades and P. Reinke, “From alloy to oxide: capturing the early stages of oxidation on Ni–Cr(100) alloys.” *ACS Appl. Mater. Interfaces*, **10**, 43219 (2018).
56. W. H. Blades, M. R. Barone, and P. Reinke, “Initial atomic-scale oxidation pathways on a Ni–15Cr(100) alloy surface.” *npj Mater. Degrad*, **5**, 1 (2021).
57. D. P. Whittle and J. Stringer, “Improvements in high temperature oxidation resistance by additions of reactive elements or oxide dispersions.” *Philos. Trans. Roy. Soc.*, **A295**, 309 (1980).
58. J. Stringer, “The reactive element effect in high temperature corrosion.” *Mat. Sci. Eng. A*, **120**, 129 (1989).
59. B. Pieraggi and R. A. Rapp, “Chromia scale growth in alloy oxidation and the reactive element effect.” *J. Electrochem. Soc.*, **140**, 2844 (1993).
60. T. L. Barth and E. A. Marquis, “Effects of minor alloying elements on alumina transformation during the transient oxidation of β-NiAl.” *Oxid. Met.*, **95**, 293 (2021).